arXiv:1704.05005v1 [cond-mat.mtrl-sci] 17 Apr 2017

# Probing electron localization by means of coalescent pairs: A simple DFT-based approach

Stefano Pittalis,[1, a)] Daniele Varsano,[1] Alain Delgado,[1, 2, 3] and Carlo Andrea Rozzi[1]
[1)] *Center S3, CNR Institute of Nanosciences, Modena, Italy*
[2)] *Department of Physics, University of Ottawa, Ottawa, Ontario K1N 6N5, Canada*
[3)] *Centro de Aplicaciones Tecnolgicas y Desarrollo Nuclear, Havana, Cuba*

The Electron Localization Function (ELF) proposed by Becke and Edgecombe is routinely adopted as a simple descriptor of atomic shells and covalent bonds. Its construction entails the information on electrons with parallel spins in single reference states and, thus, it is not a good indicator when dealing with systems as the paradigmatic case of the Hydrogen molecule. The interest in improved descriptors for the "electron localization" is also linked to the quest of improving density functional approximations. Here, we show that the ELF can be usefully complemented with the information extracted from opposite-spin correlated electron pairs by means of a procedure which, remarkably, only requires occupied Kohn-Sham orbitals. In addition to the improvements for the exemplary case of the $H_2$ molecule, we show that our approach yields appealing trends in atoms and organic molecules.

## I. INTRODUCTION

By means of the Lewis' structures, bonds can be represented in terms of shared valence electrons without any reference to the Schrödinger equation.[1] With the advent of the formalization of quantum mechanics, Valence Bond Theory expressed bonds in terms of overlapping atomic orbitals and their hybridization was necessary to account for the observed molecular geometries. As in the Lewis' structures, sharing of electrons in localized pairs is the fundamental ingredient, the simplest example of which is the covalent bond in the Hydrogen molecule ($H_2$).

Molecular Orbital Theory (MOT) provides us with an alternative picture, in which electrons occupy bonding molecular orbitals which tend to delocalize over all the nuclei in the molecule. Density Functional Theory (DFT) in its Kohn-Sham (KS) formulation replaces the central role of the interacting wave function with the electron density. Despite the fact that the electron density describes a collection of particles rather than pairs, Bader showed that a quantity such as the Laplacian of the electron density can highlight atomic shells and bonds.[2] Yet, success is not systematic and plotting is somewhat inconvenient.

Becke and Edgecombe – following another suggestion by Bader[3,4] – probed the localization of electrons by exploiting the antisymmetry of the many-electron state: if an electron is localized at a given point in space, another electron cannot be brought at the same position with the same spin. By analyzing the short-range behavior of the two-body reduced density matrix of a single reference state – i.e, an Hartree-Fock (HF) or a KS state – and taking the homogeneous gas as a reference of delocalized electrons, they could define a simple and effective Electron Localization Function (ELF).[5]

Analyses of electron localization are important also because they offer insights into possible improvements of density functional constructions.[6] Electron localization has also been connected to the ability of density functionals to access local information on the spin-entanglement,[7] to properties of the electronic stress tensor[8] and with features of time-dependent density functionals.[9] ELF, in its time-dependent extension provides a visual understanding of complex reactions involving the dynamics of excited electrons.[10] Disappointedly, however, the ELF is not adapted to visualize the bond of the Hydrogen molecule. This limitation relates to the construction of the ELF which is based on a single- rather than a multi-reference state. Fixing this problem can imply the resolution of other unsatisfactory features of the ELF. Improved approaches have been, in fact, proposed,[11–13] but at the price of departures from DFT and increased computational efforts.

*Can a useful complementation of the ELF be gained within a contained computational efforts?* Here, we give an affirmative answer by relating the electron localization to the spatial distribution of "dynamical" correlations of opposite-spin coalescent electron pairs. This implies a procedure which is applicable to any system for which *occupied* KS or HF orbitals can be computed. Tests on a variety of systems show that not only we gain a better description for $H_2$ but also improve more general features that are not optimally captured by ELF.

This manuscript is organized as follows: In Sec. II, we recall basic theoretical aspects and, after a brief introduction to the ELF, we describe the coalescent electron pair locator and tackle the problematic case of $H_2$. In Sec. III, we test our procedure for atoms, small organic molecules and the uniform electron gas. In Sec. IV, we summarize the main points, draw the conclusions, and give outlooks.

[a)] stefano.pittalis@nano.cnr.it

## II. FROM THE ELF TO THE COALESCENT PAIRS LOCATOR

The key ingredient for the derivation of the quantities we are interested in the following definitions is the distribution of electron pairs. The exact definition of the joint probability to find an electron at position $\mathbf{r}_1$ with spin $\sigma_1$ and a second electron at position $\mathbf{r}_2$ with spin $\sigma_2$ is given by:

$$P^{\sigma_1\sigma_2}(\mathbf{r}_1,\mathbf{r}_2) = N(N-1)\int d3d4..dN\,|\Psi(1,2,3,...,N)|^2\,. \tag{1}$$

where $\Psi(1,2,3,...,N)$ is the wave function of $N$ interacting electrons and $1,2,...,N$ stand for the combined spatial plus spin variables $(\mathbf{r}_1,\sigma_1),(\mathbf{r}_2,\sigma_2),...,(\mathbf{r}_N,\sigma_N)$. The calculation of this quantity for a general $N$ electron system it is not an easy task – apart from very simple cases, approximations or models are needed.

### A. ELF in a nutshell

Let us consider a wave function of the form of a *single* Salter Determinant (SD) – such as a HF or KS state. In this case, it can be easily shown that the distribution of electron pairs describes pairs of electrons that are correlated for same-spin configurations

$$P^{\sigma\sigma}_{\rm SD}(\mathbf{r}_1,\mathbf{r}_2) = \rho^{\rm SD}_\sigma(\mathbf{r}_1)\left[\rho^{\rm SD}_\sigma(\mathbf{r}_2) + h^\sigma_{\rm x}(\mathbf{r}_1,\mathbf{r}_2)\right] \tag{2}$$

but are uncorrelated for opposite spins

$$P^{\alpha\beta}_{\rm SD}(\mathbf{r}_1,\mathbf{r}_2) = \rho^{\rm SD}_\alpha(\mathbf{r}_1)\rho^{\rm SD}_\beta(\mathbf{r}_2)\,. \tag{3}$$

In Eqs. (2) and (3), $\rho^{\rm SD}$ is the electron density and $h^{\sigma\sigma}_{\rm x}(\mathbf{r}_1,\mathbf{r}_2)$ is the exchange-hole (x-hole) function

$$h^\sigma_{\rm x}(\mathbf{r}_1,\mathbf{r}_2) = -\frac{|\gamma^\sigma_{\rm SD}(\mathbf{r}_1,\mathbf{r}_2)|^2}{\rho^{\rm SD}_\sigma(\mathbf{r}_1)} \tag{4}$$

where

$$\gamma^\sigma_{\rm SD}(\mathbf{r}_1,\mathbf{r}_2) = \Sigma_i \psi^*_{i\sigma}(\mathbf{r}_1)\psi_{i\sigma}(\mathbf{r}_2)\,, \tag{5}$$

is the spin-dependent one-body reduced density matrix; here, the sum over states is restricted to occupied $\sigma$-state single-particle orbitals, $\psi_{i\sigma}$. The particle density of a single SD is obviously readily obtained from the spatial diagonal of $\gamma^\sigma_{\rm SD}$: $\rho^{\rm SD}_\sigma(\mathbf{r}) = \gamma^\sigma_{\rm SD}(\mathbf{r},\mathbf{r})$. But the particle density of a KS state equals – by construction – in the exact case, the ground state of the corresponding interacting system.

The x-hole captures the peculiar behavior of Fermions like electrons of "not liking reciprocally". Even if we admit to switch off the Coulomb repulsions, the many-electron state is antisymmetric under exchange of spatial-spin coordinates and, as a consequence, two electrons with same spin cannot sit on each other. In what follows, the information on the orientation of the electron pairs is disregarded as we only consider spherical averages, such as $f(\mathbf{r},u) := \frac{1}{4\pi}\int d\Omega_{\mathbf{u}}\; f(\mathbf{r}_1=\mathbf{r},\mathbf{r}_2=\mathbf{r}+\mathbf{u})$, where $f$ is a generic function, $d\Omega_{\mathbf{u}}$ is the element of the solid angle, and $u=|\mathbf{u}|$. Thus, the (spherical averaged) probability of finding the second electron at a distance $u$ from the first, in the limit of small $u$ vanishes as[5]

$$P^{\sigma\sigma}_{\rm SD}(\mathbf{r},u) = \frac{1}{3}D_\sigma(\mathbf{r})u^2 + \cdots\,, \tag{6}$$

where

$$D_\sigma(\mathbf{r}) := \left[\tau^{\rm SD}_\sigma(\mathbf{r}) - \frac{1}{4}\frac{\left(\nabla\rho^{\rm SD}_\sigma(\mathbf{r})\right)^2}{\rho^{\rm SD}_\sigma(\mathbf{r})}\right]\,, \tag{7}$$

and

$$\tau^{\rm SD}_\sigma(\mathbf{r}) := \Sigma_i|\nabla\psi_{i\sigma}(\mathbf{r})|^2 \tag{8}$$

is the double of the (positively defined) spin-dependent kinetic energy density.

From now on dropping the pedantic specification to a SD in our notation, Becke and Edgecombe define[5]

$$\mathrm{ELF}(\mathbf{r}) := \frac{1}{1+\chi^2_\sigma(\mathbf{r})} \tag{9}$$

where

$$\chi_\sigma(\mathbf{r}) = D_\sigma(\mathbf{r})/D^{\rm unif}_\sigma(\mathbf{r})\,, \tag{10}$$

and

$$D^{\rm unif}_\sigma(\mathbf{r}) = \frac{3}{5}\left(6\pi^2\right)^{2/3}\rho^{5/3}_\sigma(\mathbf{r}) \tag{11}$$

is evaluated for a Fermi gas at the local spin density $\rho_\sigma(\mathbf{r})$. The ELF nicely reproduces the shell structure of atoms and well emphasizes covalent bonds in molecules.[5,14]

*Disappointingly, however, the ELF is equal to 1 at every point in $H_2$ independently of the interatomic distance (because $D_\sigma(\mathbf{r})=0$).* Looking for a complementary quantity which is adapted to work for $H_2$, we shall consider electron pairs that involve opposite spins. In Sec. III, we confirm that fixing this issue for $H_2$ also implies improvements for rather different systems.

### B. Coalescent-Pair Locator

The antisymmetry of the Fermionic state does not exclude that two electrons with opposite-spins may end up on-top of each other: it is the task of the electron-electron repulsions to keep them apart. *But in the regions where atomic shells or bonds are formed, under the attraction of the nuclei, the electron-electron repulsions should be somewhat less effective for the electrons to be used as a glue: this simplified picture suggests us that it should be possible to detect electron localization by looking for*

*somewhat de-correlated singlet configurations of electron pairs*. The motion of two electrons close together is greatly influenced by the diverging electron-electron repulsion: in the parlance of multi-reference methods, this electron pair correlates "dynamically". Although, in principle, there is no clear cut between dynamical and static (non-dynamical) correlations, the general consensus is that dynamical correlations can efficiently be captured by DFT approximations. Thus, here, we proceed along a DFT-inspired approach.

Let us we define

$$\mathrm{CPL}(\mathbf{r}) := \frac{P^{\alpha\beta}(\mathbf{r}, u=0)}{P^{\alpha\beta}_{SD}(\mathbf{r}, u=0)} \, , \tag{12}$$

where CPL stands for Coalescent Pair Locator. Equation (12) involves the exact on-top distribution of interacting pairs, $P^{\alpha\beta}(\mathbf{r}, u=0)$, and, therefore, calculations turn out to be exceedingly difficult in general. The dashed black curve in Fig. 1 shows the CPL for $H_2$ at its equilibrium distance (we stress that ELF = 1 at every point). In the calculation, we employed the data of the on-top exchange and exchange-correlation holes available from Ref. 15. In doing this, we have exploited the fact that the HF and the "exact" (CI) density are practically indistinguishable – which, at the considered inter-distance of the nuclei, we have verified to be valid to a very good extent. Importantly, the *maximum* of the dashed black curve in Fig. 1 is attained in the middle along the internuclear axis where, instead, the particle density has a *minimum*: this is how a "proper" ELF should render the simplest Lewis' structure from first-principles.

In order to derive a practical and manageable expression of CPL, we start by recalling that the short range-behavior of the pair distribution is given by[16]

$$P^{\alpha\beta}(\mathbf{r}, u) = A_{\alpha\beta}(\mathbf{r})(1+u) + \cdots . \tag{13}$$

where $A_{\alpha\beta}$ is a coefficient depending on the reference point $\mathbf{r}$. Next, we replace the exact $A_{\alpha\beta}(\mathbf{r})$ with an estimation derived from a model of *dynamical* correlations. Namely, we follow a compelling proposal by Becke,[16] who constructs a spin-resolved c-hole function at coupling strength $\lambda \in [0,1]$ by implementing the picture that two electrons correlate as long as their x-holes do not screen them out. Crucially, the exact sum rule for the correlation hole (c-hole) is enforced. For the sake of simplicity, the average size of the c-hole is determined proportionally to the average size of the x-holes at each point in space. Becke's ultimate goal was the coupling averaged (DFT) quantity, but we are only interested in the fully interacting quantity ($\lambda = 1$). As a result, we obtain

$$A_{\alpha\beta}(\mathbf{r}) = \frac{\rho_\alpha(\mathbf{r})\rho_\beta(\mathbf{r})}{1 + z_{\alpha\beta}(\mathbf{r})} \tag{14}$$

where

$$z_{\alpha\beta}(\mathbf{r}) = c\left\{|U_{\mathrm{x},\alpha}(\mathbf{r})|^{-1} + |U_{\mathrm{x},\beta}(\mathbf{r})|^{-1}\right\} \, , \tag{15}$$

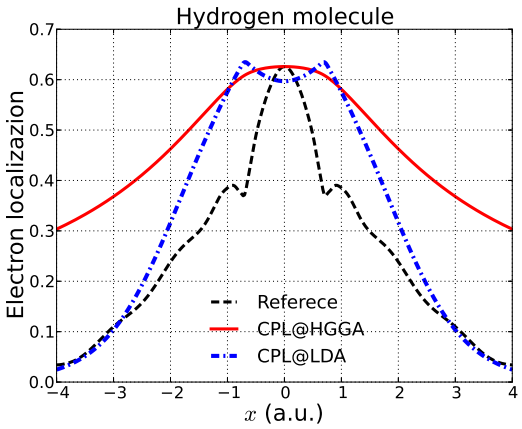


FIG. 1. Localization of the electrons expressed in terms of the CPL [Eq. (12)] for $H_2$ for a nuclear inter-distance of 1.4 a.u. at different levels of approximations. The Reference (black dashed line) is obtained by exploiting the data from Ref. 15 (see in the main text). HGGA (i.e, Hyper-GGA) (dot-dashed blue line) refers to the CPL estimated as in Eq. (17) with $c = 0.292$. HF densities calculated using Dunning gaussian basis set aug-cc-pv5Z were employed to compute the Slater potential used in Eq. (15) and Eq. (17). CPL@LDA refers to the CPL estimated according to Eq. (18).

plays the role of a correlation length, $c$ is a constant to be determined (see below), and

$$U_{\mathrm{x},\sigma}(\mathbf{r}) = \int d^3u \, \frac{h^\sigma_\mathrm{x}(\mathbf{r}, \mathbf{r}+\mathbf{u})}{u} \tag{16}$$

is the potential generated by the exchange-hole function. $U_{\mathrm{x},\sigma}$ is also known as the Slater potential or half of the spin-dependent exchange energy density in the standard gauge.[17] On passing, note that for systems with only two electrons in a singlet state, $U_{\mathrm{x},\sigma}(\mathbf{r}) = -0.5 v_\mathrm{H}(\mathbf{r})$; moreover, the DFT exchange-only and the HF solutions are, in this case, fully equivalent. Finally, we can estimate the CPL as follows:

$$\mathrm{CPL}(\mathbf{r}) \approx \frac{1}{1 + z_{\alpha\beta}(\mathbf{r})} \tag{17}$$

for any system on which we can run a DFT calculation – we also admit the additional simplification for which the Slater potential can be computed in a single-shot *post* calculation.

Fitting the DFT correlation energy of the Helium atom,[16] Becke set $c = 0.63$ in Eq. (15). For the case of the $H_2$ molecule, we realize that a value of $c = 0.292$ allows us to reproduce the maximum value of the reference case in Fig. 1. In the same figure, the dashed-dot curve in blue shows the results obtained at the level of a Local Density Approximation (LDA) using the pair distribution function of the uniform gas as parametrized in Ref. 18 and 19 – see below in Sec. III C for further details. The overall shape of the LDA is somewhat similar to the

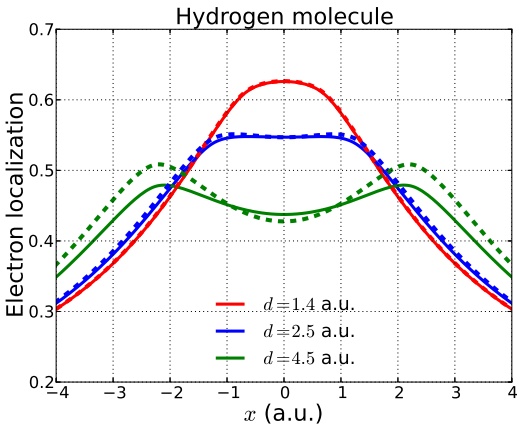


FIG. 2. Localization of the electrons expressed in terms of the CPL computed at the HGGA level according to Eq. (17) with $c = 0.292$ for $H_2$ at increasing atomic separation distance $d$. The Slater potential required as an input is obtained from HF (solid lines) and full CI (dashed-dot lines) densities. Both the HF and CI calculations employ the Dunning gaussian basis set aug-cc-pv5Z.

reference case. But, unfortunately, the desired maximum is replaced by *minimum*! This is a direct consequence of the fact that the LDA only exploits information on the particle density.

Adopting the nomenclature introduced by Perdew, we can view the expression defined in Eq. (17) as a Hyper-GGA (HGGA) form because it makes use of the Salter potential; i.e, a quantity which is proportional to the exact exchange energy density. Equation (12), however, recovers the result for the homogenous gas only in the high-density limit (more details are given below).

In Fig. 2, we follow the behavior of the CPL@HGGA as the $H_2$ bond is stretched apart. Slater potentials obtained from both HF and CI densities are employed as inputs and very similar results are obtained even at considerable internuclear distances. Yet, deviations clearly emerge due to the fact that our approach is based on a simple model that *does not* aim at including full correlations. The main point here is that the local *maximum* is eventually replaced by a local *minimum* and two different local maxima appear around each H atom. This can be intended as a clear indication of a progressive bond breaking.

## III. FURTHER ANALYSES

In this section, we illustrate other salient differences of the CPL with respect to the ELF by considering a variety of systems. This will confirm that the relevance of the CPL extends beyond the prototypical case of $H_2$.

### A. Atoms

Electrons in atoms are packed in shells. Figure 3 shows how the CPL highlights these structures in the case of the Ar atom. Near the center of the atom, electrons get squeezed in the 1s orbital and CPL $\approx 1$: this is consistent with the fact that the influence of the electron-electron interaction is weaker because of the prevalence of the nuclear attraction. Moving away from the core, the CPL exhibits a wavy behavior: this renders the idea that electrons gain some space to avoid each other but in correspondence to the shells, they tend to get together once again. It is remarkable that, although the particle density decreases monotonically and smoothly, the CPL shows some traces of the shells even at the LDA level. In systems with only one center such as atoms, the Slater potential can effectively be estimated within the BR89 approximation:[20] correspondingly, here the calculation of the CPL was stepped down from the HGGA to the Meta-GGA (MGGA) rung.

Figure 3 also shows the ELF which at a first look seems to be the champion in this case as, in fact, can detect the atomic shells rather sharply. But it seems quite artificial that an outer shells should present same or higher localization of an inner shell. The CPL, in this respect, exhibits a more compelling behavior.

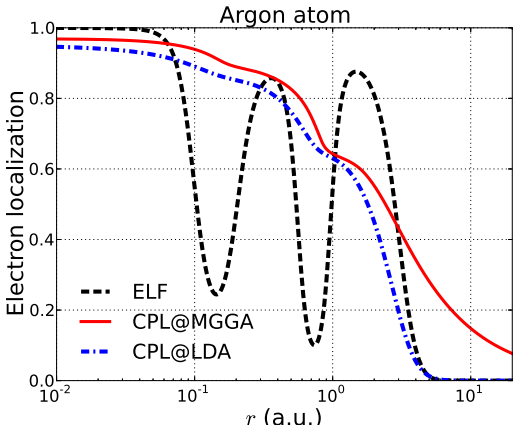


FIG. 3. Comparison of Electron localization as described in terms of the CPL and the ELF. CPL@MGGA was computed by adopting the BR89 approximation for the Slater potential[20] in Eq. (17). CPL@LDA is computed according to Eq. (18). KS@LDA results obtained by means of the APE code[21] are used as an input to all the quantities.

### B. Carbon-Carbon bonds

Let us re-consider our systems of main interest, namely molecules. The upper panel in Fig. 4 shows the CPL@HGGA for simple organic molecules – ethane, ethylene and acetylene – having respectively single, double, and triple covalent CC bonds. In the plot the $x$

axis indicates the CC bond direction. The calculations have been done using pseudo potentials, therefore the structure due to the internal electrons is "washed" out. We are here mainly interested in the structures due to the outer electrons; these are properly captured by the pseudo wavefunctions beyond the cutoff. The humps in the center highlight the presence of the bonds: the localization increases at larger bond coordination numbers. The two maxima on the side are due to the electrons of the Hydrogen atoms. For $C_2H_2$ the Hydrogen's centers are placed along the CC axis and, therefore, the electron localization results enhanced with respect to the other cases for which the Hydrogen's centers are displaced from the CC direction.

The lower panel of Fig. 4 shows the ELF for the same cases. It is apparent that the ELF, as for atoms, tends to give sharper features. But, unattractively, it assigns higher localization to bonds with lower coordination number.

Finally, we remark that our approach does not yield surface plots with different topologies for bonds with different coordination numbers as in the case for the ELF.

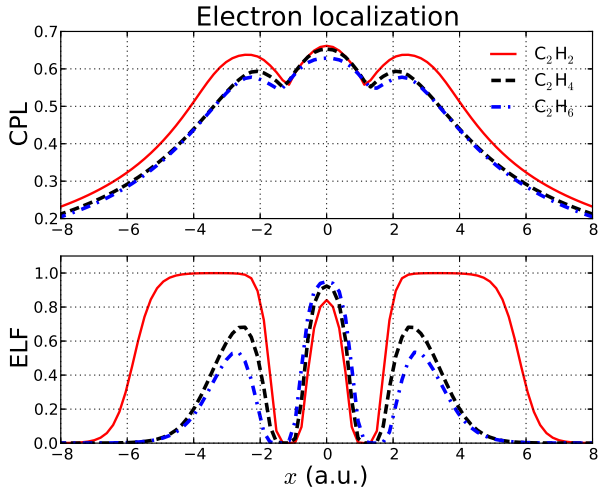


FIG. 4. Electron localization estimated in terms of the CPL (upper panel) and ELF (lower panel) for molecules having different C-C bonds at equilibrium distances. In all the cases, the CC bond is oriented along the $x$ directions. Input quantities are determined from KS@LDA results obtained by means of the Octopus code[22] in a uniform spatial grid and pseudo potentials.

### C. Uniform gas

The uniform gas allows us to derive LDAs for the CPL and to point out further aspects to be improved.

First, let us recall that the reference to the uniform gas was introduced empirically in the definition of the ELF [see Eq. (10)] in order to get meaningful plots. Thus, ELF $= 0.5$ for *any* uniform $n$.

For the uniform gas, a parametrization of the pair-correlation function is available[18] – here denoted as $g^{\alpha\beta}_{c,\mathrm{GSB}}(\mathbf{r},u)$ – to readily estimate the CPL as follows

$$\mathrm{CPL}^{\mathrm{unif}}_{\mathrm{LDA}} = 1 + g^{\alpha\beta}_{c,\mathrm{GSB}}(u=0)\,. \tag{18}$$

The aforementioned parametrization exploits Monte Carlo results and is expected to be accurate for densities corresponding to the Wigner-Seitz radius $r_s \leq 10$.

Alternatively, we may evaluate Eq. (17) with plane waves and obtain

$$\mathrm{CPL}^{\mathrm{unif}}_{\mathrm{LDA}_2} = \frac{1}{1+\frac{c}{3}(\frac{2\pi}{3})^{\frac{2}{3}} r_s}\,; \tag{19}$$

Figure 5 shows the effect of different choices for $c$. Fitting the height of the hump for $H_2$ in Fig. 1, we determined $c = 0.292$. Instead, $c = 0.630$ reproduces the DFT correlation energies for the Helium[16] and for the uniform gas, we note, improves the agreement at higher $r_s$ and better reproduces the initial slope. Obviously, there is *no* unique optimal constant $c$ – not even for the uniform gas. In general, $c$ should be intended as a density functional, whose expression should be derived beyond a simple LDA level: the search of which is postponed to future efforts.

In the high-density limit, $r_s \to 0$ and CPL $\to 1$. In the opposite limit, $r_s \to +\infty$ and CPL $\to 0$. Also note that CPL $\sim 0$ cannot be taken as an indication of locally strong interaction as this also occurs in the asymptotic region of any finite system.

As long as the uniform gas is concerned, it may be reasonable to assign higher localization to higher densities. But one may argue that the concept of localization, for this system, is more properly relate to Wigner crystallization[23,24] ($r_s \sim 106$) for which the CPL at the level of the described approximations cannot say much.

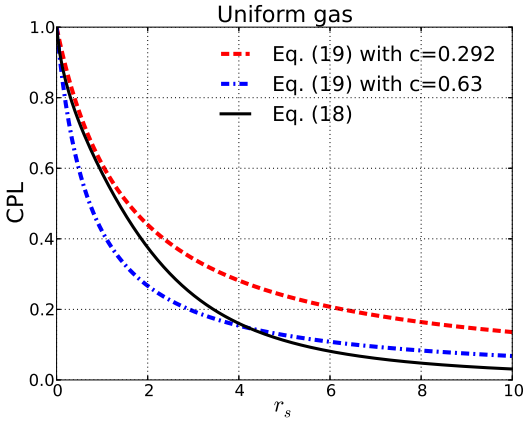


FIG. 5. Various estimations of the CPL for the uniform gas. The solid black curve provides us with an accurate reference for Wigner-Sitez radius $r_s \leq 10$.

## IV. CONCLUSIONS AND OUTLOOKS

In this work, we have presented a procedure to evaluate electron localization by detecting coalescent electron pair configurations with a relatively increased single-configuration character. Thus, we allowed ourselves to care only about *dynamical* correlations. In favor of practicality, we expressed *interacting* quantities in a post-HF fashion within an affordable computation efforts. As a result, we could resolve a few unpleasant features of the popular ELF: (i) its failure to provide any useful information for $H_2$; (ii) its tendency to assign rather high localization to outer atomic shells; and (iii) its tendency to assign *less* localization to C-C bonds with *higher* coordination number.

In this work, we mainly aimed at qualitative rather than quantitative accuracy. We pointed out, however, how the suggested procedure may be improved. Moreover, it would be interesting to evaluate the benefit of including an ability to deal with stronger correlations in the underlying model.

Bonds and shells are important inhomogeneity features in all atomistic systems, thus the interest in the evaluations of electron localization usefully links to strategies for the development of improved density functional beyond a Local Density Approximation. In this respect, our analysis contains clear hindsights on the ability of the Hyper-Generalized-Gradient-Approximation to capture static-like correlations effects by using information on the exact exchange energy densities (or, in the parlance of the present work, the Slater potential). Our analyses can also point to novel mixing for *local* hybrids schemes and partition-DFT schemes.

*Acknowledgments* – The Authors are grateful to Kieron Burke for making available data from Fig. 1 of Ref. 15. S.P. acknowledge support by the European Community through the FP7's MC-IIF MODENADYNA, grant agreement No. 623413. DV acknowledges partial support from EU Centre of Excellence MaX-Materials at the eXascale (H2020-EINFRA 2015 grant no. 676598)

[1] G. N. Lewis, Journal of the American Chemical Society **38**, 762 (1916), http://dx.doi.org/10.1021/ja02261a002.
[2] R. F. W. Bader, *Atoms in Molecules: A Quantum Theory (International Series of Monographs on Chemistry)*, 1st ed. (Clarendon Press, 1994).
[3] R. F. W. Bader and M. E. Stephens, Journal of the American Chemical Society **97**, 7391 (1975), http://dx.doi.org/10.1021/ja00859a001.
[4] R. F. W. Bader, R. J. Gillespie, and P. J. MacDougall, Journal of the American Chemical Society **110**, 7329 (1988), http://dx.doi.org/10.1021/ja00230a009.
[5] A. D. Becke and K. E. Edgecombe, The Journal of Chemical Physics **92**, 5397 (1990), http://dx.doi.org/10.1063/1.458517.
[6] M. J. P. Hodgson, J. D. Ramsden, T. R. Durrant, and R. W. Godby, Phys. Rev. B **90**, 241107 (2014).
[7] S. Pittalis, F. Troiani, C. A. Rozzi, and G. Vignale, Phys. Rev. B **91**, 075109 (2015).
[8] J. Tao, G. Vignale, and I. V. Tokatly, Phys. Rev. Lett. **100**, 206405 (2008).
[9] T. R. Durrant, M. J. P. Hodgson, J. D. Ramsden, and R. W. Godby, ArXiv e-prints (2015), arXiv:1505.07687 [cond-mat.mes-hall].
[10] T. Burnus, M. A. L. Marques, and E. K. U. Gross, Phys. Rev. A **71**, 010501 (2005).
[11] M. Kohout, K. Pernal, F. R. Wagner, and Y. Grin, Theoretical Chemistry Accounts **112**, 453 (2004).
[12] M. Kohout, K. Pernal, F. R. Wagner, and Y. Grin, Theoretical Chemistry Accounts **113**, 287 (2005).
[13] F. Feixas, E. Matito, M. Duran, M. Sol, and B. Silvi, Journal of Chemical Theory and Computation **6**, 2736 (2010), pMID: 26616075, http://dx.doi.org/10.1021/ct1003548.
[14] A. Savin, R. Nesper, S. Wengert, and T. F. Fssler, Angewandte Chemie International Edition in English **36**, 1808 (1997).
[15] K. Burke, J. P. Perdew, and M. Ernzerhof, The Journal of Chemical Physics **109**, 3760 (1998), http://dx.doi.org/10.1063/1.476976.
[16] A. D. Becke, The Journal of Chemical Physics **88**, 1053 (1988), http://dx.doi.org/10.1063/1.454274.
[17] S. Kümmel and L. Kronik, Rev. Mod. Phys. **80**, 3 (2008).
[18] P. Gori-Giorgi, F. Sacchetti, and G. B. Bachelet, Phys. Rev. B **61**, 7353 (2000).
[19] P. Gori-Giorgi, F. Sacchetti, and G. B. Bachelet, Phys. Rev. B **66**, 159901 (2002).
[20] A. D. Becke and M. R. Roussel, Phys. Rev. A **39**, 3761 (1989).
[21] M. J. Oliveira and F. Nogueira, Computer Physics Communications **178**, 524 (2008).
[22] A. Castro, H. Appel, M. Oliveira, C. A. Rozzi, X. Andrade, F. Lorenzen, M. A. L. Marques, E. K. U. Gross, and A. Rubio, physica status solidi (b) **243**, 2465 (2006).
[23] D. M. Ceperley and B. J. Alder, Phys. Rev. Lett. **45**, 566 (1980).
[24] N. D. Drummond, Z. Radnai, J. R. Trail, M. D. Towler, and R. J. Needs, Phys. Rev. B **69**, 085116 (2004).